Networks and Heterogeneous Media

https://www.aimspress.com/journal/nhm

NHM, 20(2): 387–405.
DOI: 10.3934/nhm.2025018
Received: 19 January 2025
Revised: 14 April 2025
Accepted: 21 April 2025
Published: 25 April 2025

Research article

Efficient numerical schemes for variable-order mobile-immobile advection-dispersion equation

Leqiang Zou[1,*] **and Yanzi Zhang**[2]

[1] Henan College of Industry and Information Technology, Jiaozuo, Henan 454000, China
[2] Henan Jiaozuo Normal College, Jiaozuo, Henan 454000, China

* **Correspondence:** Email: mathlq@126.com.

Abstract: In this work, we present a high-order discontinuous Galerkin (DG) method with generalized alternating numerical fluxes to solve the variable-order (VO) fractional mobile-immobile advection-dispersion equation. This equation models complex transport phenomena where the order of differentiation varies with time, providing a more accurate representation of anomalous diffusion in heterogeneous media. For spatial and temporal discretization, the method employs the DG scheme and a finite difference method, respectively. Rigorous analysis confirms that the numerical scheme is unconditionally stable and convergent. Finally, numerical experiments are conducted to validate the theoretical results and illustrate the accuracy and efficiency of the scheme.

Keywords: fractional advection-dispersion equation; time fractional derivative; complex transport phenomena; convergent

1. Introduction

Fractional differential equations (FDEs) have become an essential mathematical framework for modeling a wide range of complex phenomena, including long-range memory effects, anomalous mechanical dynamics, and advanced control processes. By generalizing classical calculus, fractional calculus enables a more accurate and flexible representation of physical systems that are inadequately captured by traditional integer-order models. This mathematical approach has been successfully applied in various disciplines, including quantitative finance, engineering, biology, chemistry, and hydrology [1, 2]. Among recent developments, variable-order (VO) fractional calculus has garnered significant attention due to its capacity to describe systems with time- or space-dependent memory characteristics and evolving dynamical behavior [3].

In recent years, a wide variety of numerical methods have been developed to solve fractional partial differential equations (FPDEs), which are often analytically intractable due to the nonlocal nature of fractional operators. Among these, finite element methods have been widely applied and rigorously analyzed for various types of time- and space-fractional models [4–8]. Finite volume methods have been adopted to handle anomalous transport and advection-diffusion processes with fractional dynamics [9–11]. Finite difference methods, known for their simplicity and effectiveness, have also been extensively investigated, with significant progress in high-order, compact, and implicit schemes [12–16]. Spectral and spectral-Galerkin methods offer highly accurate solutions and have demonstrated spectral convergence for a variety of FPDEs [17–19]. Meshless methods such as radial basis function and local interpolation approaches have emerged as powerful alternatives for multidimensional and complex-geometry problems [20–23]. Approximate analytical methods provide efficient solutions by combining analytical and numerical approaches, often using perturbation or homotopy techniques to simplify complex fractional equations [24–26]. To improve flexibility and accuracy, discontinuous Galerkin methods have been developed for both constant- and variable-order fractional equations [27–30].

The discontinuous Galerkin (DG) method combines the advantages of finite element and finite volume methods. By employing a discontinuous solution space, the DG method provides high accuracy and flexibility in solving a wide range of partial differential equations, including those with complex geometries or discontinuous solutions. This method is particularly effective for approximations of arbitrary order, making it a preferred choice for a variety of computational problems. A key strength of the DG method lies in its ability to handle adaptive meshing and high-order polynomial approximations. Furthermore, the method is supported by rigorous theoretical analysis, including error estimates and stability results.

The time-variable-order (VO) fractional mobile-immobile advection-dispersion equation effectively captures solute transport processes in porous and fractured media, providing a robust framework for studying complex migration phenomena [31–33]. A comprehensive overview of the physical background and formulation of this model is provided in [34, 35]. Sadri et al. [36] employed a spectral collocation method utilizing sixth-kind Chebyshev polynomials to solve the VO time-fractional mobile-immobile advection equations, demonstrating the efficiency and accuracy of the method. Ma et al. [37] introduced the Jacobi spectral collocation method for the variable-order advection-dispersion equation, validating its higher-order convergence through numerical analysis. Liu et al. [38] analyzed a second-order finite difference scheme for fractal mobile-immobile transport equations. Golbabai et al. [39] applied meshless methods with radial basis functions to approximate solutions for the time-fractional mobile-immobile advection-dispersion model within bounded regions. Zhang et al. [40] proposed an implicit Euler method to solve the mobile-immobile advection-dispersion model, rigorously demonstrating its unconditional stability. Jiang et al. [41] developed a numerical method based on reproducing kernel theory combined with the collocation method to address the mobile-immobile advection-dispersion model. Saffarian and Mohebbi [42] developed a robust numerical scheme for the two-dimensional time-variable-order fractional mobile-immobile advection-dispersion model, proving the unconditional stability of the fully discrete scheme.

In this paper, we propose and analyze a DG method based on generalized alternating numerical fluxes to solve the following variable-order mobile-immobile advection-dispersion equaiton

$$\begin{aligned} &c_1\omega_t + c_2 P_t^{\alpha(t)}\omega = -d_1\omega_x + d_2\omega_{xx} + g(x,t), \qquad (x,t) \in (a,b)\times(0,T], \\ &\omega(x,0) = \omega_0(x), \qquad x \in [a,b], \end{aligned} \tag{1.1}$$

where $0 < \rho(t) < 1$, $c_1 > 0$, $c_2 > 0$, and $d_1, d_2 > 0$. In this paper, g and ω_0 are assumed to be smooth functions, and the solution is considered to be either periodic or compactly supported.

The variable-order (VO) fractional derivative operator [43] is defined in the Caputo sense

$$P_t^{\rho(t)}\omega(x,t) = \frac{1}{\Gamma(1-\rho(t))}\int_0^t \frac{\partial \omega(x,s)}{\partial s}\frac{1}{(t-s)^{\rho(t)}}ds,$$

where $0 < \rho(t) < 1$.

The mobile-immobile advection-dispersion equation is a fundamental tool for describing solute transport, yet its standard formulation assumes constant-order derivatives, which may not accurately reflect the varying memory effects and heterogeneous diffusion characteristics observed in real-world systems. To address these limitations, we employ a variable-order (VO) fractional derivative, allowing the diffusion process to dynamically adapt to spatial and temporal variations in the medium. The main contributions of this paper are as follows:

(1) A high-order DG scheme with generalized alternating numerical fluxes is presented to efficiently solve the VO fractional mobile-immobile advection-dispersion equation.

(2) The stability and convergence of the proposed scheme are analyzed, ensuring its reliability for practical applications.

(3) Extensive numerical experiments are conducted to validate the theoretical findings and demonstrate the accuracy of the method for the variable-order equation.

In Section 2, the symbols, projections, and theorems required for the proof are introduced. Section 3 presents the construction of the numerical scheme for Eq (1.1) using the LDG method, and it is demonstrated that the scheme is unconditionally stable and convergent with an accuracy of $O(\Delta t + h^{k+1})$. In Section 4, numerical experiments are conducted to validate the effectiveness and reliability of the proposed scheme. Finally, the conclusions are summarized in Section 5.

2. Notations

The interval $\Omega = [a, b]$ is partitioned into subintervals, denoted by J, where $a = x_{\frac{1}{2}} < x_{\frac{3}{2}} < \cdots < x_{N+\frac{1}{2}} = b$. For $j = 1, \ldots, N$, each subinterval is defined as $I_j = [x_{j-\frac{1}{2}}, x_{j+\frac{1}{2}}]$, with the element size given by $\Delta x_j = x_{j+\frac{1}{2}} - x_{j-\frac{1}{2}}$. The maximum element size is denoted by $h = \max\limits_{1\le j\le N} \Delta x_j$.

The time interval $[0, T]$ is discretized uniformly into M time steps, such that $\Delta t = \frac{T}{M}$. The discrete time points are given as $t_n = n\Delta t$ for $n = 0, 1, \ldots, M$.

At each boundary point $x_{j+\frac{1}{2}}$, the left and right limits of the function ω are defined as $\omega^-_{j+\frac{1}{2}}$ and $\omega^+_{j+\frac{1}{2}}$, respectively. Specifically, $\omega^-_{j+\frac{1}{2}}$ corresponds to the value in the left cell I_j, while $\omega^+_{j+\frac{1}{2}}$ corresponds to the value in the right cell I_{j+1}.

The discontinuous Galerkin space V^k is defined as:

$$V^k = \{v \in P^k(I_j) : x \in I_j,\ j = 1, 2, \ldots, N\},$$

where $P^k(I_j)$ denotes the space of polynomials of degree k defined on each subinterval I_j.

In the paper, C is used to represent a positive constant, which may take different values in different cases. The inner product on $L^2(D)$ is denoted by $(\cdot,\cdot)_D$, and the associated norm is represented by $\|\cdot\|_D$. For $D = \Omega$, the subscript is omitted for simplicity.

3. The scheme

First, we introduce some lemmas that will be used to design the scheme.

Lemma 3.1. *[1] For $0 < \rho(t) < 1$ and $t > 0$, the left-sided Caputo fractional derivative is defined as*

$$ {}_0^C P_t^{\rho(t)} h(x,t) = \frac{1}{\Gamma(1-\rho(t))} \int_0^t \frac{\partial h(x,s)}{\partial s} \frac{1}{(t-s)^{\rho(t)}} \, ds, $$

is equivalent to the Riemann-Liouville fractional derivative, expressed as

$$ P_t^{\rho(t)} h(x,t) = \frac{1}{\Gamma(1-\rho(t))} \frac{d}{dt} \int_0^t \frac{h(x,s)}{(t-s)^{\rho(t)}} \, ds, $$

provided that the condition $h(x,0) = 0$ is satisfied.

Lemma 3.2. *[1] (Grünwald formula)*
The function space $\Psi^{m+a}(R)$ is defined as

$$ \Psi^{m+a}(R) = \left\{ \omega \,\middle|\, \omega \in L^1(R) : \int_{-\infty}^{\infty} (1+|\xi|)^{m+a} |\widehat{\omega}(\xi)| \, d\xi < \infty \right\}. $$

Let $\omega \in \Psi^{1+a}(R)$. It follows that

$$ \frac{1}{\Gamma(1-\rho(t))} \frac{d}{dt} \int_{-\infty}^t \frac{\omega(s)}{(t-s)^{\rho(t)}} \, ds = \frac{1}{(\Delta t)^{\rho(t)}} \sum_{j=0}^{\infty} \rho_j^{\rho(t)} \omega(t-(j-r)\Delta t) + O(\Delta t), $$

where r is an integer, and $\theta_j^{\rho(t)}$ is given by

$$ \theta_j^{\rho(t)} = (-1)^j \binom{\rho(t)}{j}. $$

The coefficients $\theta_j^{\rho(t)}$ satisfy the following properties for $0 < \rho(t) < 1$:

$$ \theta_0^{\rho(t)} = 1, \quad \theta_1^{\rho(t)} = -\rho(t) \le 0, $$

$$ \theta_2^{\rho(t)} \le \theta_3^{\rho(t)} \le \theta_4^{\rho(t)} \le \cdots \le 0, $$

$$ \sum_{k=0}^{\infty} \theta_k^{\rho(t)} = 0, \quad \sum_{k=0}^{n} \theta_k^{\rho(t)} \ge 0 \quad \text{for } n \ge 1. $$

Moreover, these coefficients can be evaluated recursively as

$$ \theta_0^{\rho(t)} = 1, \quad \theta_k^{\rho(t)} = \left(1 - \frac{\rho(t)+1}{k}\right) \theta_{k-1}^{\rho(t)} \quad \text{for } k \ge 1. $$

Lemma 3.3. *There is a constant $\sigma > 0$ such that the following condition holds:*

$$ \frac{c_2}{(\Delta t)^{\rho(t)}} \sum_{k=0}^{n-1} \theta_k^{\rho(t)} \ge \sigma > 0. $$

Let M be a positive integer, and define $t_n = \frac{n}{M}T$. The values of ω_t and $P_t^{\rho(t_n)}u$ at t_n are approximated as follows:

$$\omega_t(x,t_n) = \frac{\omega(x,t_n)-\omega(x,t_{n-1})}{\Delta t} + \gamma_1^n(x), \tag{3.1}$$

where $\gamma_1^n(x)$ represents the truncation error in the approximation of ω_t. Additionally, by applying Lemmas 3.1 and 3.2, it is obtained that

$$\begin{aligned} P_t^{\rho(t_n)}\omega(x,t_n) &= \frac{1}{\Gamma(1-\rho(t_n))}\int_0^{t_n}\frac{\partial\omega(x,s)}{\partial s}\frac{1}{(t_n-s)^{\rho(t_n)}}\,ds \\ &= \frac{1}{(\Delta t)^{\rho(t_n)}}\sum_{k=0}^{n}\theta_k^{\rho(t_n)}\omega(x,(n-k)\Delta t) + \gamma_2^n(x), \end{aligned} \tag{3.2}$$

where $\gamma_2^n(x)$ denotes the truncation error associated with the approximation of $P_t^{\rho(t_n)}\omega$. The total truncation error in the temporal direction is given by $\gamma^n(x) = \gamma_1^n(x) + \gamma_2^n(x)$, and it satisfies the bound $\|\gamma^n(x)\| \le C\Delta t$.

The problem (1.1) can be reformulated into the following system:

$$p = \omega_x, \quad c_1\omega_t + c_2P_t^{\rho(t)}\omega + d_1\omega_x - d_2p_x = g(x,t). \tag{3.3}$$

Let $\omega_h^n,\ p_h^n \in V^k$ denote the approximations of $\omega(\cdot,t_n)$ and $p(\cdot,t_n)$, respectively, and define $g^n(x) = g(x,t_n)$. The fully discrete scheme is then formulated as follows: find $\omega_h^n,\ p_h^n \in V^k$ such that, for all $v,\mu \in V^k$,

$$\begin{aligned} &\frac{c_1}{\Delta t}\int_\Omega \omega_h^n v\,dx + \frac{c_2}{(\Delta t)^{\rho(t_n)}}\theta_0^{\rho(t_n)}\int_\Omega \omega_h^n v\,dx + d_1\left(-\int_\Omega \omega_h^n v_x\,dx + \sum_{j=1}^{N}\left((\widetilde{\omega_h^n}v^-)_{j+\frac12} - (\widetilde{\omega_h^n}v^+)_{j-\frac12}\right)\right) \\ &\qquad + d_2\left(\int_\Omega p_h^n v_x\,dx - \sum_{j=1}^{N}\left((\widehat{p_h^n}v^-)_{j+\frac12} - (\widehat{p_h^n}v^+)_{j-\frac12}\right)\right) \\ &\qquad = \frac{c_1}{\Delta t}\int_\Omega \omega_h^{n-1}v\,dx + \frac{c_2}{(\Delta t)^{\rho(t_n)}}\sum_{k=1}^{n}(-\theta_k^{\rho(t_n)})\int_\Omega \omega_h^{n-k}v\,dx + \int_\Omega g^n v\,dx, \\ &\int_\Omega p_h^n\mu\,dx + \int_\Omega \omega_h^n\mu_x\,dx - \sum_{j=1}^{N}\left((\widehat{\omega_h^n}\mu^-)_{j+\frac12} - (\widehat{\omega_h^n}\mu^+)_{j-\frac12}\right) = 0. \end{aligned} \tag{3.4}$$

The hat functions in the boundary terms, which arise from the integration by parts in Eq (3.4), are referred to as numerical fluxes. The choice of an appropriate numerical flux plays a critical role in the theoretical analysis of the LDG scheme. From a practical perspective, generalized alternating numerical fluxes offer greater flexibility and broader applicability compared to traditional numerical fluxes [44]. The generalized alternating numerical fluxes are defined as follows:

$$\begin{aligned} \widehat{\omega_h^n} &= \delta(\omega_h^n)^- + (1-\delta)(\omega_h^n)^+, \\ \widehat{p_h^n} &= (1-\delta)(p_h^n)^- + \delta(p_h^n)^+, \\ \widetilde{\omega_h^n} &= \delta(\omega_h^n)^- + (1-\delta)(\omega_h^n)^+, \end{aligned} \tag{3.5}$$

where $\delta \in [0, \frac{1}{2}) \cup (\frac{1}{2}, 1]$. For $\delta = \frac{1}{2}$, the properties related to the uniqueness and approximation of the generalized Gauss-Radau projection become more intricate.

For convenience, we denote

$$\begin{aligned}\Phi_\Omega(\omega_h^n, p_h^n; \mu, v) = &\int_\Omega \omega_h^n \mu_x \, dx - \sum_{j=1}^{N} \Big(((\omega_h^n)^- \mu^-)_{j+\frac{1}{2}} - ((\omega_h^n)^- \mu^+)_{j-\frac{1}{2}} \Big) \\ &+ \int_\Omega p_h^n v_x \, dx - \sum_{j=1}^{N} \Big(((p_h^n)^+ v^-)_{j+\frac{1}{2}} - ((p_h^n)^+ v^+)_{j-\frac{1}{2}} \Big).\end{aligned} \tag{3.6}$$

To simplify the analysis, we focus on the case where $g = 0$ in the theoretic analysis.

3.1. Stability analysis

Theorem 3.1. *Suppose that $\omega(x, t) \in C([0, T], H^s(\Omega))$ with $s \geq k + 1$. Then, the fully discrete LDG scheme (3.4), with the flux (3.5), is unconditionally stable. Furthermore, ω_h^n satisfies*

$$\|\omega_h^n\| \leq \|\omega_h^0\|, \quad n = 1, 2, \ldots, M. \tag{3.7}$$

Proof. Taking $v = \omega_h^n$ and $\mu = d_2 p_h^n$ in Eq (3.4) and using the flux choice in Eq (3.5), we derive the following equation:

$$\begin{aligned}&\frac{c_1}{\Delta t}\|\omega_h^n\|^2 + \frac{c_2}{(\Delta t)^{\rho(t_n)}}\theta_0^{\rho(t_n)}\|\omega_h^n\|^2 + \frac{1}{2}d_1\sum_{j=1}^{N}[\omega_h^n]_{j-\frac{1}{2}}^2 + d_2\|p_h^n\|^2 + \Phi_\Omega(\omega_h^n, p_h^n; d_2 p_h^n, \omega_h^n) \\ &= \frac{c_1}{\Delta t}\int_\Omega \omega_h^{n-1}\omega_h^n dx + \frac{c_2}{(\Delta t)^{\rho(t_n)}}\sum_{k=1}^{n}(-\theta_k^{\rho(t_n)})\int_\Omega \omega_h^{n-k}\omega_h^n dx.\end{aligned} \tag{3.8}$$

Next, consider the cell $\mathcal{I}_j = [x_{j-\frac{1}{2}}, x_{j+\frac{1}{2}}]$. The term $\Phi_{\mathcal{I}_j}(\omega_h^n, p_h^n; d_2 p_h^n, \omega_h^n)$ is computed as:

$$\begin{aligned}\Phi_{\mathcal{I}_j}(\omega_h^n, p_h^n; d_2 p_h^n, \omega_h^n) &= d_2\Big(\int_{\mathcal{I}_j} \omega_h^n (p_h^n)_x dx - ((\omega_h^n)^-(p_h^n)^-)_{j+\frac{1}{2}} + ((\omega_h^n)^-(p_h^n)^+)_{j-\frac{1}{2}}\Big) \\ &\quad + d_2\Big(\int_{\mathcal{I}_j} p_h^n (\omega_h^n)_x dx - ((p_h^n)^+(\omega_h^n)^-)_{j+\frac{1}{2}} + ((p_h^n)^+(\omega_h^n)^+)_{j-\frac{1}{2}}\Big) \\ &= d_2\Big(((p_h^n)^-(\omega_h^n)^-)_{j+\frac{1}{2}} - ((p_h^n)^+(\omega_h^n)^+)_{j-\frac{1}{2}} \\ &\quad - ((\omega_h^n)^-(p_h^n)^-)_{j+\frac{1}{2}} + ((\omega_h^n)^-(p_h^n)^+)_{j-\frac{1}{2}} \\ &\quad - ((p_h^n)^+(\omega_h^n)^-)_{j+\frac{1}{2}} + ((p_h^n)^+(\omega_h^n)^+)_{j-\frac{1}{2}}\Big).\end{aligned} \tag{3.9}$$

By summing over $j = 1, \ldots, N$ in Eq (3.9), we observe that all boundary terms cancel out. Therefore, we have:

$$\Phi_\Omega(\omega_h^n, p_h^n; d_2 p_h^n, \omega_h^n) = 0. \tag{3.10}$$

By Lemma 3.2, we have

$$-\theta_n^{\rho(t_n)} \leq \sum_{k=0}^{n-1}\theta_k^{\rho(t_n)}. \tag{3.11}$$

Combining Eq (3.10) and the Cauchy-Schwarz inequality, Eq (3.8) becomes

$$
\begin{aligned}
&\frac{c_1}{\Delta t}\|\omega_h^n\|^2 + \frac{c_2}{(\Delta t)^{\rho(t_n)}}\theta_0^{\rho(t_n)}\|\omega_h^n\|^2 + \frac{1}{2}d_1\sum_{j=1}^{N}[\omega_h^n]_{j-\frac{1}{2}}^2 + d_2\|p_h^n\|^2 \\
&\leq \frac{c_1}{\Delta t}\|\omega_h^{n-1}\|\|\omega_h^n\| + \frac{c_2}{(\Delta t)^{\rho(t_n)}}\sum_{k=1}^{n-1}(-\theta_k^{\rho(t_n)})\|\omega_h^{n-k}\|\|\omega_h^n\| + \frac{c_2}{(\Delta t)^{\rho(t_n)}}(-\theta_n^{\rho(t_n)})\|\omega_h^0\|\|\omega_h^n\| \\
&\leq \frac{c_1}{\Delta t}\|\omega_h^{n-1}\|\|\omega_h^n\| + \frac{c_2}{(\Delta t)^{\rho(t_n)}}\sum_{k=1}^{n-1}(-\theta_k^{\rho(t_n)})\|\omega_h^{n-k}\|\|\omega_h^n\| + \frac{c_2}{(\Delta t)^{\rho(t_n)}}\sum_{k=0}^{n-1}\theta_k^{\rho(t_n)}\|\omega_h^0\|\|\omega_h^n\|,
\end{aligned}
\tag{3.12}
$$

where the last inequality uses Eq (3.11).

Dividing both sides by $\|\omega_h^n\|$, we obtain

$$
\left(\frac{c_1}{\Delta t} + \frac{c_2}{(\Delta t)^{\rho(t_n)}}\theta_0^{\rho(t_n)}\right)\|\omega_h^n\| \leq \frac{c_1}{\Delta t}\|\omega_h^{n-1}\| + \frac{c_2}{(\Delta t)^{\rho(t_n)}}\sum_{k=1}^{n-1}(-\theta_k^{\rho(t_n)})\|\omega_h^{n-k}\| + \frac{c_2}{(\Delta t)^{\rho(t_n)}}\sum_{k=0}^{n-1}\theta_k^{\rho(t_n)}\|\omega_h^0\|. \tag{3.13}
$$

To prove the theorem, we use mathematical induction.

For $n = 1$, Eq (3.13) simplifies to

$$
\|\omega_h^1\| \leq \|\omega_h^0\|. \tag{3.14}
$$

Assume that

$$
\|\omega_h^m\| \leq \|\omega_h^0\|, \quad m = 1, 2, \ldots, n-1. \tag{3.15}
$$

Using Eq (3.13), we need to prove that $\|\omega_h^n\| \leq \|\omega_h^0\|$. Substituting the inductive hypothesis into Eq (3.13), we have

$$
\begin{aligned}
&\left(\frac{c_1}{\Delta t} + \frac{c_2}{(\Delta t)^{\rho(t_n)}}\theta_0^{\rho(t_n)}\right)\|\omega_h^n\| \\
&\leq \frac{c_1}{\Delta t}\|\omega_h^0\| + \frac{c_2}{(\Delta t)^{\rho(t_n)}}\sum_{k=1}^{n-1}(-\theta_k^{\rho(t_n)})\|\omega_h^0\| + \frac{c_2}{(\Delta t)^{\rho(t_n)}}\sum_{k=0}^{n-1}\theta_k^{\rho(t_n)}\|\omega_h^0\| \\
&= \left(\frac{c_1}{\Delta t} + \frac{c_2}{(\Delta t)^{\rho(t_n)}}\theta_0^{\rho(t_n)}\right)\|\omega_h^0\|.
\end{aligned}
\tag{3.16}
$$

Dividing through by $\frac{c_1}{\Delta t} + \frac{c_2}{(\Delta t)^{\rho(t_n)}}\theta_0^{\rho(t_n)}$, we obtain

$$
\|\omega_h^n\| \leq \|\omega_h^0\|.
$$

By mathematical induction, the inequality holds for all n. Hence, the theorem is proved.

3.2. Error estimate

First, we introduce the generalized Gauss–Radau projection, which will be used in proving convergence.

For any periodic function ϖ defined on the interval $[a, b]$, the generalized Gauss-Radau projection [44], denoted by $Q_\delta\varpi$, is uniquely determined. Let $\varpi^e = Q_\delta\varpi - \varpi$ be the corresponding projection error. When $\delta \neq \frac{1}{2}$, the following conditions are satisfied for $j = 1, 2, \ldots, N$:

$$\int_{I_j} \varpi^e v\, dx = 0, \quad \forall v \in P^{k-1}(I_j), \quad \text{and} \quad (\varpi^e)^{(\delta)}_{j+\frac{1}{2}} = 0. \tag{3.17}$$

Based on these conditions, the following result can be established [44, 45].

Lemma 3.4. *Let $\delta \neq \frac{1}{2}$. If $\varpi \in H^{s+1}[a, b]$, the inequality below holds:*

$$\|\varpi^e\| + h^{\frac{1}{2}}\|\varpi^e\|_{L^2(\Gamma_h)} \leq Ch^{\min(k+1,s+1)}\|\varpi\|_{s+1}, \tag{3.18}$$

where $C > 0$ is a constant independent of h and ϖ.

Theorem 3.2. *Let $\omega(x, t) \in C([0, T], H^s(\Omega))$, with $s \geq k + 1$, denote the exact solution of the problem (1.1), and let ω_h^n represent the numerical solution obtained using the LDG scheme (3.4). The following error estimate holds*

$$\|\omega(x, t_n) - \omega_h^n\| \leq C(\Delta t + h^{k+1}),$$

where C is a constant that depends on u and T.

Proof.

$$\begin{aligned} e_\omega^n &= \omega(x, t_n) - \omega_h^n = \xi_\omega^n - \eta_\omega^n, \quad \xi_\omega^n = Q_\delta e_\omega^n, \quad \eta_\omega^n = Q_\delta\omega(x, t_n) - \omega(x, t_n), \\ e_p^n &= p(x, t_n) - p_h^n = \xi_p^n - \eta_p^n, \quad \xi_p^n = Q_{1-\delta} e_p^n, \quad \eta_p^n = Q_{1-\delta} p(x, t_n) - p(x, t_n). \end{aligned} \tag{3.19}$$

The terms η_ω^n and η_p^n are estimated using inequality (3.4).

Starting from the flux expression (3.5), with the test functions $v = \xi_\omega^n$ and $\mu = d_2\xi_p^n$, we obtain the following equation:

$$\begin{aligned} &\frac{c_1}{\Delta t}\int_\Omega (\xi_\omega^n)^2\, dx + \frac{c_2}{(\Delta t)^{\rho(t_n)}}\theta_0^{\rho(t_n)}\int_\Omega (\xi_\omega^n)^2\, dx + \frac{d_1}{2}\sum_{j=1}^{N}[\xi_\omega^n]^2_{j-\frac{1}{2}} \\ &\quad + d_2\int_\Omega (\xi_p^n)^2\, dx + \Phi_\Omega(\xi_\omega^n, \xi_p^n; d_2\xi_p^n, \xi_\omega^n) \\ &\quad = \frac{c_1}{\Delta t}\int_\Omega \eta_\omega^n\xi_\omega^n\, dx + \frac{c_2}{(\Delta t)^{\rho(t_n)}}\theta_0^{\rho(t_n)}\int_\Omega \eta_\omega^n\xi_\omega^n\, dx \\ &\quad + d_2\int_\Omega \eta_p^n\xi_p^n\, dx - \frac{c_1}{\Delta t}\int_\Omega \eta_\omega^{n-1}\xi_\omega^n\, dx - \int_\Omega \gamma^n(x)v\, dx \\ &\quad + \Phi_\Omega(\eta_\omega^n, \eta_p^n; d_2\xi_p^n, \xi_\omega^n) + \frac{c_2}{(\Delta t)^{\rho(t_n)}}\sum_{k=1}^{n}(-\theta_k^{\rho(t_n)})\int_\Omega \xi_\omega^{n-k}\xi_\omega^n\, dx \\ &\quad - \frac{c_2}{(\Delta t)^{\rho(t_n)}}\sum_{k=1}^{n}(-\theta_k^{\rho(t_n)})\int_\Omega \eta_\omega^{n-k}\xi_\omega^n\, dx. \end{aligned} \tag{3.20}$$

Using properties (3.17), it follows that

$$\Phi_\Omega(\eta_\omega^n, \eta_p^n; d_2\xi_p^n, \xi_\omega^n) = 0.$$

Next, applying Eqs (3.10) and (3.11), and the Cauchy-Schwarz inequality, the following inequality is obtained

$$\begin{aligned}
&\frac{c_1}{\Delta t}\|\xi_\omega^n\|^2 + \frac{c_2}{(\Delta t)^{\rho(t_n)}}\theta_0^{\rho(t_n)}\|\xi_\omega^n\|^2 + \frac{d_1}{2}\sum_{j=1}^{N}[\xi_\omega^n]_{j-\frac{1}{2}}^2 + d_2\|\xi_p^n\|^2 \\
&\le \frac{c_1}{\Delta t}(\|\eta_\omega^n\| + \|\eta_\omega^{n-1}\|)\|\xi_\omega^n\| + \frac{c_1}{\Delta t}\|\xi_\omega^{n-1}\|\|\xi_\omega^n\| + \|\gamma^n(x)\|\|\xi_\omega^n\| \\
&+ \frac{c_2}{(\Delta t)^{\rho(t_n)}}\sum_{k=1}^{n-1}(-\theta_k^{\rho(t_n)})\|\xi_\omega^{n-k}\|\|\xi_\omega^n\| + \frac{c_2}{(\Delta t)^{\rho(t_n)}}\sum_{k=0}^{n-1}\theta_k^{\rho(t_n)}\|\xi_\omega^0\|\|\xi_\omega^n\| \\
&+ \frac{c_2}{(\Delta t)^{\rho(t_n)}}\sum_{k=1}^{n-1}(-\theta_k^{\rho(t_n)})\|\eta_\omega^{n-k}\|\|\xi_\omega^n\| + \frac{c_2}{(\Delta t)^{\rho(t_n)}}\sum_{k=0}^{n-1}\theta_k^{\rho(t_n)}\|\eta_\omega^0\|\|\xi_\omega^n\| \\
&+ \frac{c_2}{(\Delta t)^{\rho(t_n)}}\theta_0^{\rho(t_n)}\|\eta_\omega^n\|\|\xi_\omega^n\| + d_2\|\eta_p^n\|\|\xi_p^n\|.
\end{aligned} \tag{3.21}$$

Using the estimate

$$\left\|\frac{\eta_\omega^i - \eta_\omega^{i-1}}{\Delta t}\right\| \le \left\|\frac{1}{\Delta t}\int_{t_{i-1}}^{t_i}\frac{\partial}{\partial t}(Q_\delta\omega(x,t) - \omega(x,t))\right\| \le Ch^{k+1}\|\omega_t\|_{L^\infty(H^2(\Omega))},$$

we obtain

$$\int_\Omega\left(\frac{\eta_\omega^n - \eta_\omega^{n-1}}{\Delta t}\right)\xi_\omega^n\,dx \le Ch^{k+1}\|\omega_t\|_{L^\infty(H^2(\Omega))}\|\xi_\omega^n\|,$$

and thus, we have the following inequality:

$$\begin{aligned}
&\frac{c_1}{\Delta t}\|\xi_\omega^n\|^2 + \frac{c_2}{(\Delta t)^{\rho(t_n)}}\theta_0^{\rho(t_n)}\|\xi_\omega^n\|^2 + \frac{d_1}{2}\sum_{j=1}^{N}[\xi_\omega^n]_{j-\frac{1}{2}}^2 + d_2\|\xi_p^n\|^2 \\
&\le \Bigg(\frac{c_1}{\Delta t}(\|\eta_\omega^n\| + \|\eta_\omega^{n-1}\|) + \frac{c_1}{\Delta t}\|\xi_\omega^{n-1}\| + \|\gamma^n(x)\| \\
&+ \left(\frac{c_2}{(\Delta t)^{\rho(t_n)}}\sum_{k=1}^{n-1}(-\theta_k^{\rho(t_n)})\right)(\|\xi_\omega^{n-k}\| + \|\eta_\omega^{n-k}\|) \\
&+ \left(\frac{c_2}{(\Delta t)^{\rho(t_n)}}\sum_{k=0}^{n-1}\theta_k^{\rho(t_n)}\right)(\|\xi_\omega^0\| + \|\eta_\omega^0\|) \\
&+ \frac{c_2}{(\Delta t)^{\rho(t_n)}}\theta_0^{\rho(t_n)}\|\eta_\omega^n\|\Bigg)\|\xi_\omega^n\| + d_2\|\eta_p^n\|\|\xi_p^n\|.
\end{aligned} \tag{3.22}$$

There exists a constant $\chi > 0$ such that

$$-(\theta_1^{\rho(t_n)} + \theta_2^{\rho(t_n)} + \cdots + \theta_{n-1}^{\rho(t_n)}) \le \theta_0^{\rho(t_n)} \le -\chi(\theta_1^{\rho(t_n)} + \theta_2^{\rho(t_n)} + \cdots + \theta_{n-1}^{\rho(t_n)}),$$

using Lemma 3.3 and noticing the fact that

$$ab \le \varepsilon a^2 + \frac{1}{4\varepsilon}b^2, a \in R, b \in R, \varepsilon > 0. \tag{3.23}$$

Let $k=\frac{c_1}{\Delta t}+\frac{c_2}{(\Delta t)^{\rho(t_n)}}\theta_0^{\rho(t_n)}$, and then we use the fact (3.23) twice, first let

$$\begin{aligned}
a=&\Bigg(\frac{c_1}{\Delta t}(\|\eta_\omega^n\|+\|\eta_\omega^{n-1}\|)+\frac{c_1}{\Delta t}\|\xi_\omega^{n-1}\|+\|\gamma^n(x)\|\\
&+\left(\frac{c_2}{(\Delta t)^{\rho(t_n)}}\sum_{k=1}^{n-1}(-\theta_k^{\rho(t_n)})\right)(\|\xi_\omega^{n-k}\|+\|\eta_\omega^{n-k}\|)\\
&+\left(\frac{c_2}{(\Delta t)^{\rho(t_n)}}\sum_{k=0}^{n-1}\theta_k^{\rho(t_n)}\right)(\|\xi_\omega^0\|+\|\eta_\omega^0\|)\\
&+\frac{c_2}{(\Delta t)^{\rho(t_n)}}\theta_0^{\rho(t_n)}\|\eta_\omega^n\|\Bigg),\\
b=&\|\xi_\omega^n\|,\quad \varepsilon=\frac{k}{2}>0,
\end{aligned}$$

then let $a=\|\eta_p^n\|, b=\|\xi_p^n\|, \varepsilon=\frac{1}{2}$. Since

$$\left(\frac{c_2}{(\Delta t)^{\rho(t_n)}}\sum_{k=1}^{n-1}\chi(-\theta_k^{\rho(t_n)})\right)\geq\left(\frac{c_2}{(\Delta t)^{\rho(t_n)}}\theta_0^{\rho(t_n)}\right),$$

so

$$\frac{c_2}{(\Delta t)^{\rho(t_n)}}\theta_0^{\rho(t_n)}\|\eta_\omega^n\|\leq\chi\left(\frac{c_2}{(\Delta t)^{\rho(t_n)}}\sum_{k=1}^{n-1}(-\theta_k^{\rho(t_n)})\right)\|\eta_\omega^n\|,$$

then the inequality (3.22) becomes

$$\begin{aligned}
\frac{k}{2}\|\xi_\omega^n\|^2\leq&\frac{1}{2k}\Bigg(\frac{c_1}{\Delta t}(\|\eta_\omega^n\|+\|\eta_\omega^{n-1}\|)+\frac{c_1}{\Delta t}\|\xi_\omega^{n-1}\|\\
&+\left(\frac{c_2}{(\Delta t)^{\rho(t_n)}}\sum_{k=1}^{n-1}(-\theta_k^{\rho(t_n)})\right)(\|\xi_\omega^{n-k}\|+\|\eta_\omega^{n-k}\|+\chi\|\eta_\omega^n\|)\\
&+\left(\frac{c_2}{(\Delta t)^{\rho(t_n)}}\sum_{k=0}^{n-1}\theta_k^{\rho(t_n)}\right)(\|\xi_\omega^0\|+\|\eta_\omega^0\|+\frac{1}{\sigma}\|\gamma^n(x)\|)\Bigg)^2\\
&+\frac{d_2}{2}\|\eta_p^n\|^2.
\end{aligned}\tag{3.24}$$

By the fact that

$$a^2+b^2\leq(a+b)^2,\quad ab\geq 0,$$

multiplying Eq (3.24) by $2k$, and let

$$\begin{aligned}
a=&\frac{c_1}{\Delta t}(\|\eta_\omega^n\|+\|\eta_\omega^{n-1}\|)+\frac{c_1}{\Delta t}\|\xi_\omega^{n-1}\|\\
&+\left(\frac{c_2}{(\Delta t)^{\rho(t_n)}}\sum_{k=1}^{n-1}(-\theta_k^{\rho(t_n)})\right)(\|\xi_\omega^{n-k}\|+\|\eta_\omega^{n-k}\|+\chi\|\eta_\omega^n\|)\\
&+\left(\frac{c_2}{(\Delta t)^{\rho(t_n)}}\sum_{k=0}^{n-1}\theta_k^{\rho(t_n)}\right)(\|\xi_\omega^0\|+\|\eta_\omega^0\|+\frac{1}{\sigma}\|\gamma^n(x)\|),\\
b=&\sqrt{d_2k}\|\eta_p^n\|,
\end{aligned}$$

we can obtain the following inequality:

$$
\begin{aligned}
k\|\xi_\omega^n\| \le{}& \frac{c_1}{\Delta t}(\|\eta_\omega^n\| + \|\eta_\omega^{n-1}\|) + \frac{c_1}{\Delta t}\|\xi_\omega^{n-1}\| \\
&+ \left(\frac{c_2}{(\Delta t)^{\rho(t_n)}}\sum_{k=1}^{n-1}(-\theta_k^{\rho(t_n)})\right)(\|\xi_\omega^{n-k}\| + \|\eta_\omega^{n-k}\| + \chi\|\eta_\omega^n\|) \\
&+ \sqrt{d_2 k}\|\eta_p^n\| + \left(\frac{c_2}{(\Delta t)^{\rho(t_n)}}\sum_{k=0}^{n-1}\theta_k^{\rho(t_n)}\right)(\|\xi_\omega^0\| + \|\eta_\omega^0\| + \frac{1}{\sigma}\|\gamma^n(x)\|).
\end{aligned}
\tag{3.25}
$$

When $n = 1$, Eq (3.25) becomes

$$
\begin{aligned}
\left(\frac{c_1}{\Delta t} + \frac{c_2}{(\Delta t)^{\rho(t_1)}}\theta_0^{\rho(t_1)}\right)\|\xi_\omega^1\| \le{}& \frac{c_1}{\Delta t}\left(\|\eta_\omega^1\| + \|\eta_\omega^0\|\right) + \frac{c_1}{\Delta t}\|\xi_\omega^0\| + \sqrt{d_2 k}\|\eta_p^1\| \\
&+ \left(\frac{c_2}{(\Delta t)^{\rho(t_1)}}\theta_0^{\rho(t_1)}\right)\left(\|\xi_\omega^0\| + \|\eta_\omega^0\| + \frac{1}{\sigma}\|\gamma^1(x)\|\right).
\end{aligned}
\tag{3.26}
$$

Note that $\|\xi_\omega^0\| = 0$, and from Eq (3.4), we obtain

$$
\|\xi_\omega^1\| \le C(\Delta t + h^{k+1}). \tag{3.27}
$$

We assume that the inequality holds for all $m = 1, 2, \ldots, n-1$, that is

$$
\|\xi_\omega^m\| \le C(\Delta t + h^{k+1}). \tag{3.28}
$$

It is noted that

$$
\frac{c_2}{(\Delta t)^{\rho(t_n)}}\sum_{k=0}^{n-1}\theta_k^{\rho(t_n)} + \frac{c_2}{(\Delta t)^{\rho(t_n)}}\sum_{k=1}^{n-1}(-\theta_k^{\rho(t_n)}) = \frac{c_2}{(\Delta t)^{\rho(t_n)}}\theta_0^{\rho(t_n)}.
$$

From Eqs (3.25) and (3.28), the following inequality is obtained:

$$
\begin{aligned}
\left(\frac{c_1}{\Delta t} + \frac{c_2}{(\Delta t)^{\rho(t_n)}}\theta_0^{\rho(t_n)}\right)\|\xi_\omega^n\| \le{}& \frac{c_1}{\Delta t}C(\Delta t + h^{k+1}) \\
&+ \frac{c_2}{(\Delta t)^{\rho(t_n)}}\sum_{k=1}^{n-1}(-\theta_k^{\rho(t_n)})C(\Delta t + h^{k+1}) \\
&+ \frac{c_2}{(\Delta t)^{\rho(t_n)}}\sum_{k=0}^{n-1}\theta_k^{\rho(t_n)}C(\Delta t + h^{k+1}).
\end{aligned}
\tag{3.29}
$$

Thus, we conclude that

$$
\|\xi_\omega^n\| \le C(\Delta t + h^{k+1}).
$$

Finally, by applying the triangle inequality and the interpolation property, the proof of Theorem 3.2 is completed.

4. Numerical experiment

Example 4.1. Consider the problem (1.1) with parameters $c_1 = 1$, $c_2 = 2$, $d_1 = 1$, $d_2 = 2$, and the initial condition $u(x, 0) = 0$. The function $g(x, t)$ is defined as

$$g(x,t) = 2t\sin(2\pi x) + \frac{4t^{2-\rho(t)}}{\Gamma(3-\rho(t))}\sin(2\pi x) + 2\pi t^2\cos(2\pi x) + 4\pi^2 t^2\sin(2\pi x).$$

The exact solution for this problem is given by $\omega(x, t) = t^2 \sin(2\pi x)$.

The spatial convergence properties of the scheme (3.4) are evaluated using this example. The temporal step size is fixed at $\Delta t = 1/1000$, while the spatial mesh sizes are varied as $h = 1/5$, $1/10$, $1/15$, and $1/20$, respectively. The resulting numerical errors and convergence rates in both the L^2-norm and L^∞-norm, corresponding to various fractional orders, are presented in Tables 1 and 2. It is evident that the proposed scheme achieves the optimal convergence rates when using piecewise P^k polynomial.

By fixing a sufficiently small spatial mesh size $h = \frac{1}{500}$ and choosing various temporal step sizes $\Delta t = \frac{1}{5}, \frac{1}{10}, \frac{1}{20}, \frac{1}{40}$, we observe from Table 3 that the numerical results exhibit a first-order convergence in time, which is consistent with our theoretical results.

To further validate the accuracy of the proposed high-order DG method, we perform a comparison with a finite difference (FD) method for solving the variable-order fractional advection-dispersion Eq (1.1) with the same parameters and the initial condition. We first divide the spatial domain $[a, b]$ into N equal subintervals with mesh size $h_1 = \frac{b-a}{N}$, and denote $x_j = a + jh_1$, for $j = 0, 1, \ldots, N$. We approximate the spatial derivatives of $\omega(x, t_n)$ at the grid points x_j using finite differences as follows:

$$\begin{aligned} \omega_x(x_j,t_n) &\approx \frac{\omega(x_{j+1},t_n)-\omega(x_j,t_n)}{h_1}, \\ \omega_{xx}(x_j,t_n) &\approx \frac{\omega(x_{j+1},t_n)-2\omega(x_j,t_n)+\omega(x_{j-1},t_n)}{h_1^2}. \end{aligned} \tag{4.1}$$

Substitute Eqs (4.1), (3.1) and (3.2) into the original equation, we obtain the fully discrete scheme

$$\begin{aligned} &\frac{c_1}{\Delta t}\left(\omega_j^n - \omega_j^{n-1}\right) + \frac{c_2}{(\Delta t)^{\rho(t_n)}}\sum_{k=0}^{n}\theta_k^{\rho(t_n)}\omega_j^{n-k} \\ &= -d_1\cdot\frac{\omega_{j+1}^n-\omega_{j-1}^n}{2h_1} + d_2\cdot\frac{\omega_{j+1}^n-2\omega_j^n+\omega_{j-1}^n}{h_1^2} + g_j^n, \end{aligned} \tag{4.2}$$

where

- $\omega_j^n \approx \omega(x_j, t_n)$,
- $g_j^n = g(x_j, t_n)$ is the known source term,
- $\theta_k^{\rho(t_n)}$ are weights from the fractional convolution quadrature,
- γ_j^n is the total truncation error at (x_j, t_n), satisfying $\|\gamma_j^n\| \le C(\Delta t + h_1^2)$.

The variable fractional order is chosen as $\rho(t) = \frac{8-t}{15}$.

In the comparison, we fix the time step as $\Delta t = 1/1000$ and vary the spatial mesh size $h_1 = 1/10, 1/20, 1/30, 1/40$. The numerical errors and observed convergence rates in the L^2-norm for both the DG method (using piecewise P^1 polynomials) and the FD method (4.2) are shown in Figure 1. It is observed that both methods exhibit second-order convergence in space now. However, the DG method demonstrates higher accuracy than the finite difference scheme. Moreover, the DG method is capable of achieving $(k+1)$-th order spatial convergence when using piecewise P^k polynomials. For example, third-order convergence is attained with piecewise P^2 polynomials, as evidenced by the results in Tables 1 and 2.

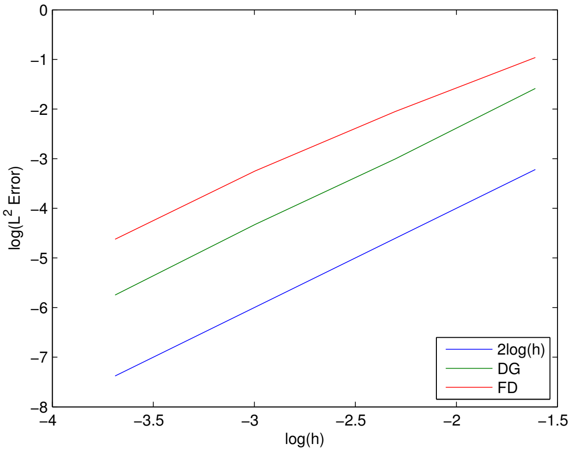

Figure 1. Error in L^2 norm for DG method (using piecewise P^1 polynomials) and the FD method (4.2), $\rho(t) = \frac{8-t}{15}$.

Table 1. Spatial accuracy test when taking piecewise P^k polynomials using generalized numerical fluxes on uniform meshes for $\rho(t) = \frac{e^t+1}{5}$, $\Delta t = 1/1000$, $\delta = 0.6$, $T = 1$.

$\rho(t)$	P^k	N	L^∞-error	order	L^2-error	order
$\rho(t) = \frac{e^t+1}{5}$	P^0	5	0.781356543644563	-	0.811643551435544	-
		10	0.390678271822282	1.00	0.431944597464271	0.91
		15	0.260452181214854	0.92	0.298665460272027	0.92
		20	0.195339135911141	0.97	0.229874475006395	0.89
	P^1	5	0.365454345536453	-	0.413153543451345	-
		10	0.093283329546276	1.97	0.109937078106140	1.91
		15	0.041966645713413	1.92	0.050676881906131	1.94
		20	0.023810852648272	1.92	0.029253436970555	1.97
	P^2	5	0.025342434342468	-	0.032634552345326	-
		10	0.003466508284447	2.87	0.004341905554260	2.91
		15	0.001082705465106	2.82	0.001334304063205	2.91
		20	0.000474172272630	2.91	0.000577674350873	2.92

Table 2. Spatial accuracy test when taking piecewise P^k polynomials using generalized numerical fluxes on uniform meshes for $\rho(t) = \frac{\sin t+2}{10}$, $\Delta t = 1/1000$, $\delta = 0.2$, $T = 1$.

$\rho(t)$	P^k	N	L^∞-error	order	L^2-error	order
$\rho(t) = \frac{\sin t+2}{10}$	P^0	5	0.543432507028769	-	0.732453465895323	-
		10	0.292479082134599	0.92	0.367236212865906	0.95
		15	0.197158461423066	0.93	0.247942026683542	0.94
		20	0.148119129679174	0.96	0.187525639215507	0.90
	P^1	5	0.386745645464365	-	0.429856341235466	-
		10	0.092682012633183	1.87	0.099368444058785	1.98
		15	0.039432065256851	1.82	0.045507256764390	1.94
		20	0.021259111655579	1.92	0.023036687278259	1.91
	P^2	5	0.035464563245658	-	0.042325479864524	-
		10	0.006003059928863	2.85	0.007044728419360	2.90
		15	0.002187236794468	2.92	0.002564554191487	2.94
		20	0.001058292464021	2.91	0.001241791511304	2.92

Table 3. Temporal errors and convergence rates for piecewise linear P^1 basis functions when $\Delta t = 1/1000$, $\delta = 0.3$, $T = 1$.

	M	L^2-error	order	L^∞-error	order
$\rho(t) = \frac{(\cos t)^2}{15-2t}$	5	0.135345464564645	-	0.093453566456722	-
	10	0.067198735409812	1.01	0.046712374092112	1.03
	20	0.032480178908534	1.04	0.022305479807943	1.05
	40	0.016432954718745	0.98	0.010942573201284	1.07
$\rho(t) = \frac{1+e^t}{10}$	5	0.134556576878564	-	0.114547748454358	-
	10	0.061872654328745	1.10	0.055431287635421	1.02
	20	0.029389751008234	1.05	0.026058974358762	0.97
	40	0.014032178945671	1.01	0.012462398754123	1.08

Example 4.2. To illustrate the impact of different variable-order fractional derivatives, we consider the initial condition:

$$\omega(x, 0) = \sin(\pi x), \quad x \in [0, 1].$$

We solve the variable-order mobile-immobile advection-dispersion equation (1.1) using two different choices for the fractional order function:

- Case 1: A linear function, $\rho(t) = 0.8 - 0.3t$.
- Case 2: An exponential function, $\rho(t) = 0.6e^{-0.5t}$.

The final time is set to $T = 1$, and the computed solutions are plotted in Figure 2. We can observe

- The solution with linear order $\rho(t) = 0.8 - 0.3t$ leads to a gradual decrease in diffusion, resulting in a smoother and more spread-out profile.

- The solution with exponential order $\rho(t) = 0.6e^{-0.5t}$ exhibits initially strong diffusion that slows down over time, leading to a more localized concentration of the solution.
- This comparison highlights how different variable-order fractional derivatives influence the dispersion behavior, with lower orders leading to slower diffusion and more localized effects.

These results demonstrate the flexibility of variable-order fractional models in capturing complex transport phenomena, making them more suitable for describing real-world diffusion processes compared to classical integer-order models.

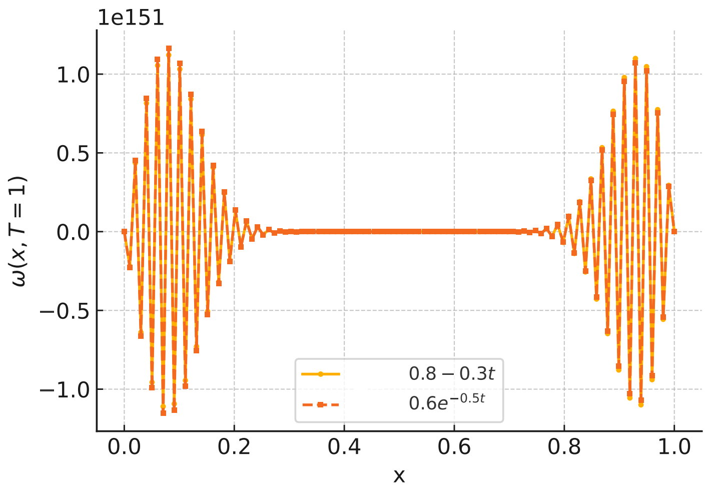

Figure 2. Numerical solutions at $T = 1$ for different fractional orders.

5. Conclusions

In this study, a high-order numerical method is introduced for solving the time-variable-order fractional mobile-immobile advection-dispersion model. The proposed scheme combines the finite difference method with the local discontinuous Galerkin (LDG) method. Through the careful selection of projections and numerical fluxes, it is demonstrated that the scheme is unconditionally stable and achieves a convergence rate of $O(\Delta t + h^{k+1})$ in the L^2 norm.

It is worth noting that while this work focuses on the time-fractional model, the method could also be extended to handle fractional derivatives with respect to the spatial variable, as explored in [46]. The numerical scheme and stability analysis would require modifications to accommodate the nonlocal nature of spatial fractional derivatives, which will be considered in our future work.

Author contributions

L. Zou wrote the main manuscript text. Y. Zhang analyzed the stability and convergence of the scheme. All authors reviewed the manuscript.

Use of AI tools declaration

The authors declare they have not used Artificial Intelligence (AI) tools in the creation of this article.

Conflict of interest

The authors declare there is no conflict of interest.

References

1. I. Podlubny, *Fractional Differential Equations*, Academic Press, 1999.
2. W. Deng, Smoothness and stability of the solutions for nonlinear fractional differential equations, *Nonlinear Anal. Theory Methods Appl.*, **72** (2010), 1768–1777. https://doi.org/10.1016/j.na.2009.09.018
3. Q. Li, Y. Chen, Y. Huang, Y. Wang, Two-grid methods for nonlinear time fractional diffusion equations by L1-Galerkin FEM, *Math. Comput. Simul.*, **185** (2021), 436–451. https://doi.org/10.1016/j.matcom.2020.12.033
4. X. Zheng, H. Wang, Optimal-order error estimates of finite element approximations to variable-order time-fractional diffusion equations without regularity assumptions of the true solutions, *IMA J. Numer. Anal.*, **41** (2021), 1522–1545. https://doi.org/10.1093/imanum/draa013
5. Y. Zhao, C. Shen, M. Qu, W. P. Bu, Y. F. Tang, Finite element methods for fractional diffusion equations, *Int. J. Model., Simul., Sci. Comput.*, **11** (2020), 2030001. https://doi.org/10.1142/S1793962320300010
6. X. Li, H. Rui, Two temporal second-order H^1-Galerkin mixed finite element schemes for distributed-order fractional sub-diffusion equations, *Numerical Algorithms*, **79** (2018), 1107–1130. https://doi.org/10.1007/s11075-018-0476-4
7. W. Bu, A. Xiao, W. Zeng, Finite difference/finite element methods for distributed-order time fractional diffusion equations, *J. Sci. Comput.*, **72** (2017), 422–441. https://doi.org/10.1007/s10915-017-0360-8
8. L. Feng, P. Zhuang, F. Liu, I. Turner, Y. Gu, Finite element method for space-time fractional diffusion equation, *Numerical Algorithms*, **72** (2016), 749–767. https://doi.org/10.1007/s11075-015-0065-8
9. A. J. Cheng, H. Wang, K. X. Wang, A Eulerian-Lagrangian control volume method for solute transport with anomalous diffusion, *Numer. Methods Partial Differ. Equ.*, **31** (2015), 253–267. https://doi.org/10.1002/num.21901
10. M. Badr, A. Yazdani, H. Jafari, Stability of a finite volume element method for the time-fractional advection-diffusion equation, *Numer. Methods Partial Differ. Equ.*, **34** (2018), 1459–1471. https://doi.org/10.1002/num.22243
11. F. Liu, P. Zhuang, I. Turner, K. Burrage, V. Anh, A new fractional finite volume method for solving the fractional diffusion equation, *Appl. Math. Modell.*, **38** (2014), 3871–3878. https://doi.org/10.1016/j.apm.2013.10.007
12. M. Stynes, E. O'Riordan, J. Gracia, Error analysis of a finite difference method on graded meshes for a time-fractional diffusion equation, *SIAM J. Numer. Anal.*, **55** (2017), 1057–1079. https://doi.org/10.1137/16M1082329

13. R. Choudhary, S. Singh, P. Das, D. Kumar, A higher-order stable numerical approximation for time-fractional non-linear Kuramoto-Sivashinsky equation based on quintic B-spline, *Math. Methods Appl. Sci.*, **47** (2024), 1–23. https://doi.org/10.1002/mma.9778

14. X. M. Gu, H. W. Sun, Y. L. Zhao, X. C. Zheng, An implicit difference scheme for time-fractional diffusion equations with a time-invariant type variable order, *Appl. Math. Lett.*, **120** (2021), 107270. https://doi.org/10.1016/j.aml.2021.107270

15. X. D. Zhang, Y. L. Feng, Z. Y. Luo, J. Liu, A spatial sixth-order numerical scheme for solving fractional partial differential equation, *Appl. Math. Lett.*, **159** (2025), 109265. https://doi.org/10.1016/j.aml.2024.109265

16. Y. Feng, X. Zhang, Y. Chen, L. Wei, A compact finite difference scheme for solving fractional Black-Scholes option pricing model, *J. Inequal. Appl.*, **36** (2025), 36. https://doi.org/10.1186/s13660-025-03261-2

17. C. Li, F. Zeng, F. Liu, Spectral approximations to the fractional integral and derivative, *Fract. Calc. Appl. Anal.*, **15** (2012), 383–406. doi.org/10.2478/s13540-012-0028-x

18. S. Guo, L. Mei, Z. Zhang, Y. Jiang, Finite difference/spectral-Galerkin method for a two-dimensional distributed-order time-space fractional reaction-diffusion equation, *Appl. Math. Lett.*, **85** (2018), 157–163. https://doi.org/10.1016/j.aml.2018.06.005

19. X. Li, C. Xu, A space-time spectral method for the time fractional diffusion equation, *SIAM J. Numer. Anal.*, **47** (2009), 2108–2131. https://doi.org/10.1137/080718942

20. A. Bhardwaj, A. Kumar, A meshless method for time fractional nonlinear mixed diffusion and diffusion-wave equation, *Appl. Numer. Math.*, **160** (2021), 146–165. https://doi.org/10.1016/j.apnum.2020.09.019

21. Y. Gu, H. G. Sun, A meshless method for solving three-dimensional time fractional diffusion equation with variable-order derivatives, *Appl. Math. Modell.*, **78** (2020), 539–549. https://doi.org/10.1016/j.apm.2019.09.055

22. V. R. Hosseini, E. Shivanian, W. Chen, Local integration of 2-D fractional telegraph equation via local radial point interpolant approximation, *Eur. Phys. J. Plus*, **130** (2015), 33. https://doi.org/10.1140/epjp/i2015-15033-5

23. Z. Avazzadeh, W. Chen, V. R. Hosseini, The coupling of RBF and FDM for solving higher order fractional partial differential equations, *Appl. Mech. Mater.*, **598** (2014), 409–413. https://doi.org/10.4028/www.scientific.net/AMM.598.409

24. P. Das, S. Rana, H. Ramos, A perturbation-based approach for solving fractional-order Volterra-Fredholm integro-differential equations and its convergence analysis, *Int. J. Comput. Math.*, **97** (2020), 1994–2014. https://doi.org/10.1080/00207160.2019.1673892

25. P. Das, S. Rana, H. Ramos, Homotopy perturbation method for solving Caputo-type fractional-order Volterra-Fredholm integro-differential equations, *Comput. Math. Methods*, **1** (2019), e1047. https://doi.org/10.1002/cmm4.1047

26. P. Das, S. Rana, H. Ramos, On the approximate solutions of a class of fractional order nonlinear Volterra integro-differential initial value problems and boundary value problems of first kind and their convergence analysis, *J. Comput. Appl. Math.*, **404** (2022), 113116. https://doi.org/10.1016/j.cam.2020.113116
27. L. Wei, Y. F. Yang, Optimal order finite difference/local discontinuous Galerkin method for variable-order time-fractional diffusion equation, *J. Comput. Appl. Math.*, **383** (2021), 113129. https://doi.org/10.1016/j.cam.2020.113129
28. L. Wei, W. Li, Local discontinuous Galerkin approximations to variable-order time-fractional diffusion model based on the Caputo-Fabrizio fractional derivative, *Math. Comput. Simul.*, **188** (2021), 280–290. https://doi.org/10.1016/j.matcom.2021.04.001
29. W. Li, L. Wei, Analysis of Local Discontinuous Galerkin Method for the Variable-order Subdiffusion Equation with the Caputo-Hadamard Derivative, *Taiwanese J. Math.*, **28** (2024), 1095–1110. https://doi.org/10.11650/tjm/240801
30. Y. Liu, M. Zhang, H. Li, J. Li, High-order local discontinuous Galerkin method combined with WSGD-approximation for a fractional sub-diffusion equation, *Comput. Math. Appl.*, **73** (2017), 1298–1314. https://doi.org/10.1016/j.camwa.2016.08.015
31. B. P. Moghaddam, J. A. T. Machado, Extended algorithms for approximating variable order fractional derivatives with applications, *J. Sci. Comput.*, **71** (2016), 1351–1374. https://doi.org/10.1007/s10915-016-0343-1
32. L. Ramirez, C. Coimbra, On the selection and meaning of variable order operators for dynamic modeling, *Int. J. Differ. Equ.*, **2010** (2010), 1–16. https://doi.org/10.1155/2010/846107
33. Z. Chen, J. Z. Qian, H. B. Zhan, L. W. Chen, S. H. Luo, Mobile-immobile model of solute transport through porous and fractured media, *IAHS Publ.*, **341** (2011), 154–158.
34. R. Schumer, D. A. Benson, M. M. Meerschaert, B. Baeumer, Fractal mobile/immobile solute transport, *Water Resour. Res.*, **39** (2003), 1–12. https://doi.org/10.1029/2003WR002141
35. Y. Zhang, D. A. Benson, D. M. Reeves, Time and space nonlocalities underlying fractional-derivative models: Distinction and literature review of field applications, *Adv. Water Resour.*, **32** (2009), 561–581.
36. K. Sadri, H. Aminikhah, An efficient numerical method for solving a class of variable-order fractional mobile-immobile advection-dispersion equations and its convergence analysis, *Chaos, Solitons Fractals*, **146** (2021), 110896. https://doi.org/10.1016/j.chaos.2021.110896
37. H. Ma, Y. Yang, Jacobi spectral collocation method for the time variable-order fractional mobile-immobile advection-dispersion solute transport model, *East Asian J. Appl. Math.*, **6** (2016), 337–352. https://doi.org/10.4208/eajam.141115.060616a
38. Z. G. Liu, A. J. Cheng, X. L. Li, A second order finite dfference scheme for quasilinear time fractional parabolic equation based on new fractional derivative, *Int. J. Comput. Math.*, **95** (2017), 396–411. https://doi.org/10.1080/00207160.2017.1290434
39. A. Golbabai, O. Nikan, T. Nikazad, Numerical investigation of the time fractional mobile-immobile advection-dispersion model arising from solute transport in porous media, *Int. J. Appl. Comput. Math.*, **5** (2019), 1–22. https://doi.org/10.1007/s40819-019-0635-x

40. H. Zhang, F. Liu, M. S. Phanikumar, M. M. Meerschaert, A novel numerical method for the time variable fractional order mobile-immobile advection-dispersion model, *Comput. Math. Appl.*, **66** (2013), 693–701. https://doi.org/10.1016/j.camwa.2013.01.031

41. W. Jiang, N. Liu, A numerical method for solving the time variable fractional order mobile-immobile advection-dispersion model, *Appl. Numer. Math.*, **119** (2017), 18–32. https://doi.org/10.1016/j.apnum.2017.03.014

42. M. Saffarian, A. Mohebbi, An efficient numerical method for the solution of 2D variable order time fractional mobile-immobile advection-dispersion model, *Math. Methods Appl. Sci.*, **44** (2021), 5908–5929. https://doi.org/10.1002/mma.7158

43. C. F. M. Coimbra, Mechanica with variable-order differential operators, *Ann. Phys.*, **12** (2003), 692–703. https://doi.org/10.1002/andp.200351511-1203

44. Y. Cheng, X. Meng, Q. Zhang, Application of generalized Gauss-Radau projections for the local discontinuous Galerkin method for linear convection-diffusion equations, *Math. Comp.*, **86** (2017), 1233–1267. https://doi.org/10.1090/mcom/3141

45. L. Wei, H. Wang, Y. Chen, Local discontinuous Galerkin method for a hidden-memory variable order reaction-diffusion equation, *J. Appl. Math. Comput.*, **69** (2023), 2857–2872. https://doi.org/10.1007/s12190-023-01865-9

46. W. Wang, E. Barkai, Fractional advection-diffusion-asymmetry equation, *Phys. Rev. Lett.*, **125** (2020), 240606. https://doi.org/10.1103/PhysRevLett.125.240606

AIMS Press